

ARMY RESEARCH LABORATORY



Sound Exposure Calculations for Transient Events and Other
Improvements to an Acoustical Tactical Decision Aid

D. Keith Wilson, V. Anh Nguyen, Nassy Srour, and John Noble

ARL-TR-2757

August 2002

Approved for public release; distribution unlimited.

20021017 073

The findings in this report are not to be construed as an official Department of the Army position unless so designated by other authorized documents.

Citation of manufacturer's or trade names does not constitute an official endorsement or approval of the use thereof.

Destroy this report when it is no longer needed. Do not return it to the originator.

Army Research Laboratory

Adelphi, MD 20783-1197

ARL-TR-2757

August 2002

Sound Exposure Calculations for Transient Events and Other Improvements to an Acoustical Tactical Decision Aid

D. Keith Wilson, John Noble

Computational and Information Sciences Directorate

V. Anh Nguyen, Nassy Srour

Sensors and Electron Devices Directorate

Sponsored by

National Ground Intelligence Center
220 Seventh Street NE
Charlottesville, VA 22902-5396

Abstract

Recent enhancements to an acoustical tactical decision aid, called the Acoustic Battlefield Aid (ABFA), are described. ABFA predicts the effects of the atmosphere and local terrain on the performance of acoustical sensors, using advanced sound propagation models. Among the enhancements are (1) sound-exposure and detection calculations for moving and transient sources, (2) new display capabilities including loading of vector-map features from CDs, (3) an interactive menu for entering and managing acoustical and meteorological ground properties, (4) initialization of runs from field trials stored in the U.S. Army Research Laboratory's Automatic Target Recognition Acoustic Database, (5) a Java-based interface to numerical weather forecast data over the Internet, and (6) creation of a Windows executable version using the MATLAB compiler.

Contents

1	Introduction	1
2	Display Enhancements	2
2.1	Display Formats and Options	2
2.2	Display Rotation	3
2.3	Positioning of the Calculation Domain	4
2.4	Map Backgrounds from Vector Format Geographic Data	4
3	Initialization from the ATR Database	7
4	Spectral Representations	11
5	Moving and Transient Sources	14
5.1	Internal Representation of Nonstationary Sources	14
5.2	Calculation Method for Nonstationary Sources	15
5.3	Moving Source Implementation	17
5.4	Transient Source Implementation	18
6	Java Weather Interface	23
7	Dependence of Sound Speed on Atmospheric Humidity	25
8	Ground Parameter Menu	29
9	Creation of an ABFA Windows Executable	31
10	Concluding Remarks and Future Recommendations	33

Figures

1	Map for the Annapolis, MD area generated from VMAP0 vector features and DTED terrain elevations.	6
2	ABFA display after initialization from ATR Acoustic Database file apg8_36. The path of a ground vehicle driving on Spesutie Island (APG, MD) is shown. The starting point of the path is indicated by an x and the ending point by an arrow. Positions of acoustic sensors are indicated by circles.	9
3	ABFA display after initialization from ATR Acoustic Database file apg8_66. The path of a helicopter flying over the Aberdeen, MD area is shown. See Figure 2 for legend.	10
4	Probability of detection display for a moving source. White represents high probability of detection; medium gray represents near-zero probability of detection.	19
5	Three representations for shock waves and explosions. Plotted is $p(t)/A$, where A is the peak overpressure. The time axis is normalized by the positive phase duration T_p	20
6	Ground parameter menu.	30

1. Introduction

The Acoustic Battlefield Aid (ABFA) is a tactical decision aid providing the capability to predict and simulate performance of battlefield acoustical sensors. It can also be used to predict noise impacts from military activities. ABFA combines advanced models for sound propagation in the atmosphere with a library of source representations and algorithms for assessing sensor performance. Important propagation effects, such as refraction by atmospheric wind and temperature gradients, signal coherence reduction from atmospheric turbulence, and shadowing by terrain features and buildings, are included in the calculations. Early versions of ABFA were described in two technical reports. The first (Wilson 1998) described the basic organization and physical models used by the program. The second (Wilson and Szeto 2000) described the user interface, object representations, and some tools designed to enhance functionality.

The present technical report describes several recent enhancements to ABFA that are part of the new Version 3.0. These features include the ability to perform calculations with transient and moving sources, access to various sources of weather data over the Internet, map displays with geographic features from CD-ROMs produced by the National Imagery and Mapping Agency (NIMA), and an informative ground parameter display allowing users to create and name their own ground types. The report also describes how a Windows executable version of ABFA was created from its MATLAB (The MathWorks, Inc. 2000) source code using the MATLAB compiler and function libraries.

One of the most significant enhancements in ABFA Version 3.0 is the ability to simulate the performance user-supplied detection and beamforming algorithms. A separate technical report by Wilson et al. (2002) describes this new capability.

2. Display Enhancements

Many graphical enhancements are present in the new version of ABFA. Three basic types of displays are now available along with options for customizing them. Rotation of the display is easily done with the mouse, and convenient new tools for positioning the computational domain have been developed.

2.1 Display Formats and Options

Previous versions of ABFA (specifically Versions 2.5 and 2.6) allowed two primary types of displays: a color image representing the calculation values (or terrain elevations) could be overlaid on either a 3-D mesh plot or a 2-D georectified, pixelized map background (.jpeg or .gif format). The new version of ABFA, 3.0, adds a third type of display, in which the user creates his/her own map background using vectorized map features found on CD-ROMs produced by NIMA. This type of display is discussed in more detail later.

Although the appearance of the three of the primary display types may seem very different, they are all created in a similar manner. Technically, each display type consists of a color surface plot above a layer of miscellaneous objects whose characteristics are customized by the user. MATLAB's **FaceAlpha** (transparency) property of the surface plot and the **EraseMode** property of the underlying miscellaneous objects are changed to achieve the desired displays. For example, to create the 3-D mesh plot, the surface's **FaceAlpha** is normally set to 1, which produces an opaque plot. The view angle is set from the side to create the 3-D appearance. To create an overlay on a map background, the surface's **FaceAlpha** value is set to 0.5, which creates a semi-transparent plot. The surface mesh lines are erased and the map background is placed on the layer below the surface. Setting the view angle overhead, a 2-D, map-style plot is produced. In the vector-map feature mode, the user-selected features are plotted on the lower layer with the **EraseMode** property set to "none". This setting allows the features to be seen even when the **FaceAlpha** property of the color surface is set to 1.

Users can add grid and elevation lines from the display options dialog box, which is accessed from the Display pull-down menu. Terrain elevations below a user-specified elevation (set to 0 m by default) can be colored blue

to suggest water if desired. A contour plot of the current calculation quantity can be also be added to the display. On the 3-D mesh plot, the contours are visible on a flat surface underneath the mesh. These contours are usually partially obstructed by the overlying mesh. (The display can be rotated to see the contours more clearly.) For the map background displays, the color surface is made partially transparent by default, so as not to obscure the contours. To create pure contour plots, the overlying surface may be made invisible from the display options dialog box by selecting “Make color display image fully transparent.”

With regard to the display of geographic information, it should be noted that the ABFA graphical display and calculations are rectilinear, thereby being based on the flat-earth assumption. This is entirely reasonable for the envisioned applications of the program, which involve areas of roughly 20×20 km or less. Although the user can choose to display and enter coordinates in relative (easting and northing from a fixed origin at the southwest corner of the display), UTM (Universal Transverse Mercator), and latitude/longitude coordinate systems, the graphical display and calculations are always based on the relative coordinates. For example, in the latitude/longitude system, ABFA simply produces linear axes interpolating between the latitude and longitude of the southwest and northeast corners of the display. The display still shows relative positions based on a flat-earth assumption; only the axes labels are changed. When positions of an object are entered in a latitude/longitude system, ABFA first converts the coordinates to UTM (WGS-84) coordinates. It then subtracts the UTM coordinates of the origin (southwest corner) from the object’s coordinates to determine the relative coordinates. The resulting relative coordinates are subsequently used for display and calculations. Entry of coordinates in a UTM system simply omits the first step in this procedure. When working with UTM coordinates, ABFA determines the grid zone based on the location of the origin.

2.2 Display Rotation

A significant change in the new version of ABFA that will be immediately evident to users of previous versions is the removal of the slider bars controlling the azimuth and elevation view angles. The slider bars have been replaced by the “Enable Display Rotation/Disable Selection” command on the ABFA Display pull-down menu. When the user enables rotation from the pull-down menu, or presses Ctrl-R, the display enters a rotation mode where the view angles can be adjusted by clicking on the terrain display with the mouse and then dragging. In the rotation mode, the current mouse position is indicated by a “fleur” symbol (perpendicular,

double arrows). A 3-D outline box, indicating the extent of the terrain mesh, is displayed during the dragging process. The numerical values of the azimuth and elevation appear in the lower left corner of the window. When the view angles have been set as desired, the user should select “Disable Display Rotation/Enable Selection” from the Display pull-down menu or press Ctrl-R. This returns ABFA to the source/receiver selection mode, where a mouse click on a source or receiver selects it for a calculation. In the selection mode, the mouse position is indicated by a standard pointing arrow.

2.3 Positioning of the Calculation Domain

Several methods for positioning the computational domain can be accessed from the Terrain pull-down menu. The first of these (which was the only one available in previous versions), involves specifying the latitude/longitude or UTM coordinates of the southwest and northeast corners the domain. An alternative method now available is for the user to first specify the locations of sources and/or receivers of interest, and then have ABFA automatically choose the southwest and northeast corners of the domain so that all sources and receivers are visible with a suitable margin around the edge of the display. In addition, the Digital Chart of the World's (DCW's) Gazetteer can be searched for place names. (The DCW Gazetteer contains more than 100,000 place names, with an emphasis on names of cities and major airports. It is distributed with ABFA, so that users need not obtain their own CD-ROM.) To use this capability, the user specifies a search string. All matches found in the DCW Gazetteer are then listed. Once the user has selected the desired match from the list, ABFA retrieves the latitude/longitude coordinates from the Gazetteer and then centers the computational domain on this location.

Once the calculation domain has been set, the user can zoom in/out and reposition the center of the display by selecting “Zoom In/Out and Translate Domain” from the Terrain pull-down menu. The user specifies values for the zoom factors and translations in km for the easterly and northerly coordinates. If the display includes terrain elevations [from Digital Terrain Elevation Data (DTED) CDs provided by NIMA] and vector map features, the user is prompted to insert the CDs so ABFA can load geographic data for the new display location.

2.4 Map Backgrounds from Vector Format Geographic Data

As mentioned earlier, the new version of ABFA can display geographic objects found on NIMA CDs. Both the Vector Map Level 0 (VMAP0)

format and its predecessor, DCW, are supported through functions found in the MATLAB Mapping Toolbox. These CDs contain features in several different themes, including political boundaries, population centers, roads, railways, airports, rivers, lakes, and coastlines. ABFA users can exercise control over which of these themes are displayed from the “Show Geographic Objects” dialog box accessed through the Display pull-down menu.

ABFA internally sets the colors to use for the various map features:

- Rivers are plotted as thin, medium blue lines.
- Coastal boundaries are plotted as thick, medium blue lines.
- Roads and railways are plotted as thin, black lines.
- Airports are plotted as open black squares.
- Political boundaries are plotted as thick, white lines.
- The outlines of population centers are plotted as medium width, gray lines.

An example vector-feature map background for the Annapolis, MD area is shown in Figure 1. A 20×20 km region is shown. This map was generated from the NIMA VMAP0 and DTED level 1 CDs. The city limits for Annapolis are indicated by gray lines near the center of the map. The Chesapeake Bay is to the east. Major roadways, including part of the Bay Bridge, are indicated as solid lines. Locations of surface weather stations (which are maintained by ABFA in a separate file) appear as white triangles. A close look at the display suggests that the outline of Annapolis is not correctly positioned on the peninsula between the Severn and Magothy Rivers, being shifted somewhat to the south and west. This occurs because the VMAP0 coordinates have an accuracy of several hundred meters and therefore do not always line up well with the more precise DTED level 1 coverage.

When users “right-click” on the map features, a description of the feature pops up. These descriptions, which are taken from the NIMA CDs, often do not provide information as specific as desired. For example, U.S. Interstate 95 would carry the generic description “Primary or secondary roads or highways; Functional” when loaded from DCW. If desired, the object may be renamed by clicking on the description, thereby opening a property dialog box. The string property for the object (its name) can then be changed. Text annotations may also be added to the map from the Display pull-down menu. The word “Annapolis” in Figure 1 was added in this way, because the VMAP0 CDs (unlike the DCW CDs) do not include place names.

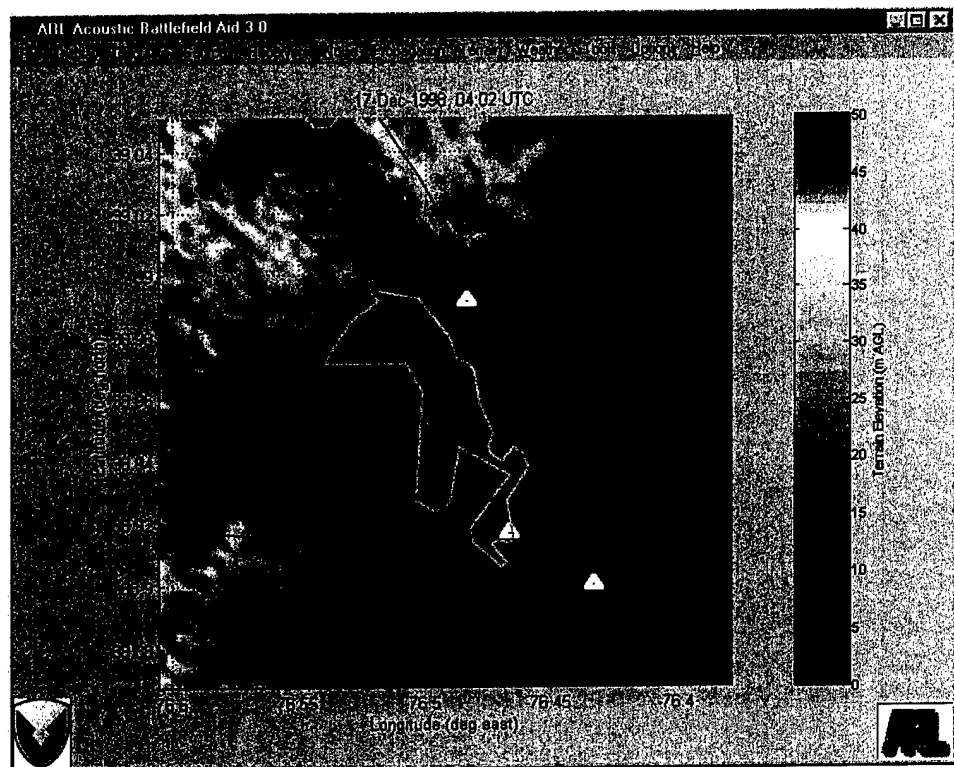


Figure 1. Map for the Annapolis, MD area generated from VMAP0 vector features and DTED terrain elevations.

3. Initialization from the ATR Database

The U.S. Army Research Laboratory (ARL) has collected a large database of acoustic signatures, primarily from trials conducted at Aberdeen Proving Ground (APG), MD. The signatures are stored in a binary format, together with Global Positioning System (GPS) data for the target and sensor positions, target descriptions, sensor characteristics, weather conditions, and a classification of the local ground type. These files have been assembled with a set of graphical and analysis tools, together creating the Automatic Target Recognition (ATR) Acoustic Database/Laboratory (Nguyen et al. 1999).

A capability has been developed to initialize ABFA runs with trials from the ATR Acoustic Database. Three types of files are used:

1. The GPS target coordinate file, titled `xxxx_t.gps`, where “xxxx” is the field campaign designation (e.g., `apg5` for the fifth set of trials conducted at APG) and “t” is the trial number. This file has a text format, generally with four columns: time (24-hr clock), UTM northing, UTM easting, and height above ground level. The height column is sometimes omitted. Each line in the file represents the target coordinates at a different time. Multiple vehicles may be stored sequentially in the GPS file. Each vehicle appears as a separate block, with blocks separated by a blank line.
2. The GPS sensor coordinate (survey) file, titled `xxxx.sur`. This text file contains the UTM coordinates (northing followed by easting) for each sensor in the field campaign. A self-contained array of microphones is considered to be a single sensor. The coordinates of each sensor is listed on a separate line.
3. The header file(s), titled `xxxx_t_s.hdr`. Here “s” is the sensor number. The header files are unique for each trial and sensor, containing the day of year, time of day, the target type(s), the array configuration, microphone calibrations (in some cases), the weather and ground conditions, and other information.

A run is initialized from the ATR Acoustic Database by selecting “Configure ABFA from ATR Database Files” from the Tools pull-down menu. ABFA first prompts for the name of the GPS target coordinate (.gps) file. An ABFA moving source representation is then created from the

information in this file. Next, coordinates of the receiver(s) are loaded from the related survey (.sur) file. ABFA then performs a search for all available .hdr files from the trial. It loads the target type, day of year, time of day, and weather and ground conditions from the first available file. An attempt is made to find a close match between the target type and available target representations in the ABFA library, although this is not always possible. The array configurations are then loaded from each of the available .hdr files. As for the targets, ABFA attempts to find a match between the array configuration and the available receiver representations. The last step in the process is to redraw the display and update the internal ABFA settings to reflect this new information. As a part of this process, terrain elevations and vector feature map data can be loaded if desired.

Some example ABFA initializations from the ATR Acoustic Database are shown in Figures 2 and 3. Both of these trials were conducted in the Aberdeen, MD area on 17 December 1998. Figure 2, which is for trial apg8_36, shows the path of a ground vehicle on Spesutie Island, APG, MD. The initial position of the vehicle is marked by an X and the final position by an arrow. Positions of sensors during the trial are indicated by circles. The second Figure, 3, is the flight path of a helicopter.

In the future, the capability to initialize ABFA runs from the ATR Acoustic Database should provide excellent opportunities for verifying ABFA predictions.

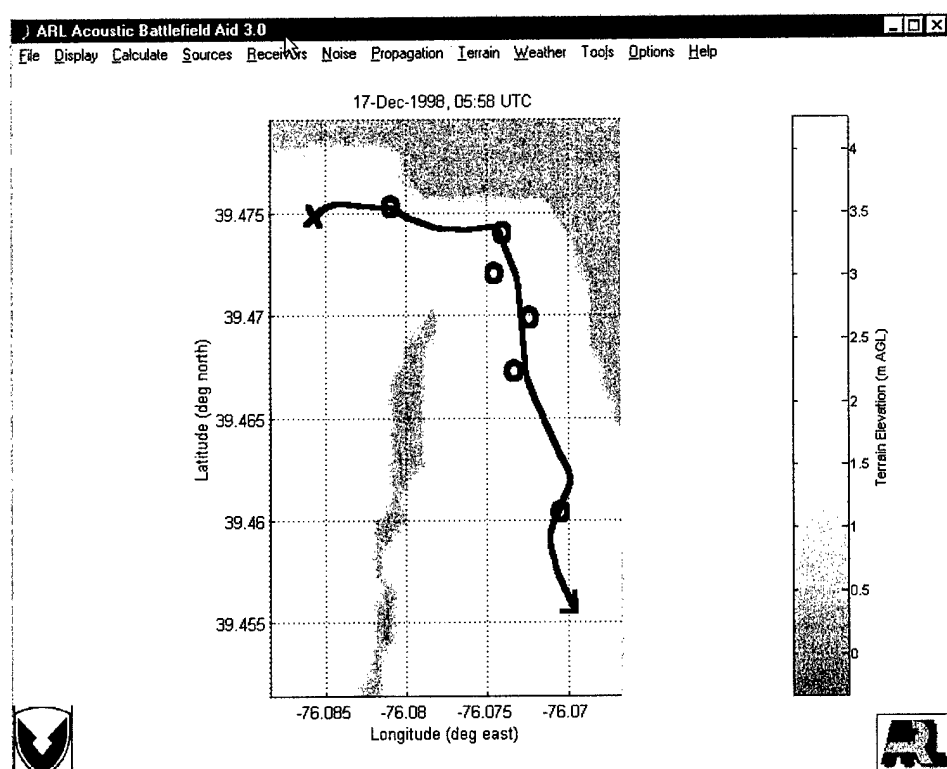


Figure 2. ABFA display after initialization from ATR Acoustic Database file apg8.36. The path of a ground vehicle driving on Spesutie Island (APG, MD) is shown. The starting point of the path is indicated by an x and the ending point by an arrow. Positions of acoustic sensors are indicated by circles.

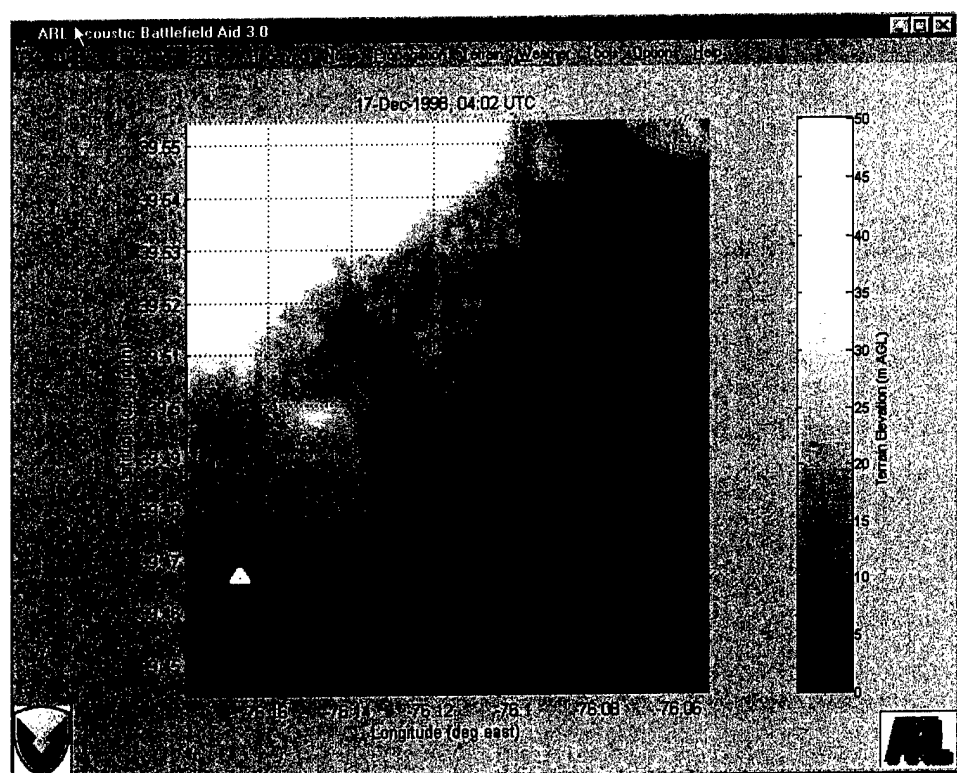


Figure 3. ABFA display after initialization from ATR Acoustic Database file apg8-66. The path of a helicopter flying over the Aberdeen, MD area is shown. See Figure 2 for legend.

4. Spectral Representations

ABFA performs its propagation calculations in the frequency domain. As described in an earlier technical report (Wilson and Szeto 2000), the frequency-domain representation for the acoustic sources and background noise is composed of finite-width bands, each band having a power-law dependence on frequency. Designating the overall power spectral density as $S(f)$ (where f is frequency) and the power spectral density in each band as $S_n(f)$, the representation can be written mathematically as

$$S(f) = \sum_{n=1}^N S_n(f), \quad (1)$$

where

$$S_n(f) = \begin{cases} A_n f^{p_n}, & f_{\ell,n} \leq f < f_{u,n} \\ 0, & \text{elsewhere.} \end{cases} \quad (2)$$

In these equations, $f_{\ell,n}$ is the lower-frequency bound for band n , $f_{u,n}$ is the upper-frequency bound, A_n is the spectral coefficient, and p_n is the power-law exponent. The spectral densities are assumed to be derived from sound-pressure signals that have been normalized $p_{\text{ref}} = 20 \mu\text{Pa}$, the standard reference pressure for aeroacoustics. Therefore, the actual units of the spectral densities are seconds.

Internally, ABFA implements the spectral representations as MATLAB structures containing four fields: `LowFreq`, `HighFreq`, `SpecSlope`, and `loudness`. In the standard representation, these fields are each arrays with N elements, containing the $f_{\ell,n}$, the $f_{u,n}$, the p_n , and the sound-pressure levels (SPLs) L_n . Here L_n is obtained by integrating equation (2) across the frequency band:

$$L_n = 10 \log \int_{f_{\ell,n}}^{f_{u,n}} S_n(f) df = \begin{cases} 10 \log \left[A_n (p_n + 1) \left(f_{u,n}^{p_n+1} - f_{\ell,n}^{p_n+1} \right) \right], & p_n \neq -1 \\ 10 \log [A_n \ln (f_{u,n}/f_{\ell,n})], & p_n = -1. \end{cases} \quad (3)$$

The units of L_n are dB re 20 μPa .

In addition, three representations alternative to the standard one are provided: 1/3-octave band, octave band, and Fast Fourier Transform

(FFT) bin coefficients. The last of these was added to ABFA Version 3 to support calculations with transient source emissions. Internally, the currently active representation is indicated by the field `OctaveBand`, which has a value of 0 for the standard representation, 1 for 1/3-octave-band levels, 2 for octave band levels, and -1 for FFT bin coefficients. The various representations and conversions between them are described in the following.

- *Octave-Band Representation.* Two frequencies are spaced by an octave when the higher one is double the lower. In the ABFA octave-band representation, the value stored in the `loudness` field is the value of L_n that would be observed if the frequency limits of the band were expanded or contracted such that this frequency doubling condition is met. The power-law exponent p_n is always -1 in the octave-band representation. Because the SPL for $p_n = -1$ is given by the equation $L_n = 10 \log [A_n \ln (f_{u,n}/f_{\ell,n})]$, the corresponding octave-band level would be $L_{\text{oct}} = 10 \log (A_n \ln 2)$. Equating the A_n s, we find

$$L_n = L_{\text{oct}} + 10 \log \left[\frac{\ln (f_{u,n}/f_{\ell,n})}{\ln 2} \right]. \quad (4)$$

- *1/3-Octave-Band Representation.* This representation is the same as for octave bands, except that the `loudness` field stores the value of L_n that would be observed if the frequency limits of the band were expanded or contracted such that the higher frequency is $2^{1/3}$ times the lower. The resulting equation relating the standard level to the 1/3-octave level is

$$L_n = L_{1/3} + 10 \log \left[\frac{\ln (f_{u,n}/f_{\ell,n})}{\ln 2^{1/3}} \right]. \quad (5)$$

- *FFT Bin Coefficients.* The bin coefficients represent the Fourier transform of the pressure signal recorded at a microphone, normalized by p_{ref} . They are complex values so that the full time series can be reconstructed. Only the first $M/2 + 1$ coefficients (where M is the length of the time series) need be stored due to the symmetry inherent to the transform of a real series. Denoting the sampling rate as f_s , the lower frequencies of the bins are $f_{\ell,n} = (n - 1)(f_s/M)$ and the upper frequencies are $f_{u,n} = n(f_s/M)$. The power-law exponent p_n is always 0 in the bin coefficient representation. Assuming the input signal is normalized by p_{ref} , the FFT bin coefficients Y_n are related to the sound power levels by

$$L_n = 20 \log_{10} |Y_n|. \quad (6)$$

Note that the L_n s can be derived uniquely from the Y_n s, but not vice-versa, due to the signal phase information in the Y_n s.

ABFA's Acoustic Waveform Analysis User Interface [(AWAUI), see Wilson and Szeto (2000)] was extended to support the FFT bin coefficient representation. When called with the `OctaveBand` field set to -1 , the user may switch between displays of the time series and power spectrum. When AWAUI is called with one of the other representations, the time series display is disabled because it cannot be reconstructed without the signal phase information.

5. Moving and Transient Sources

Previous versions of ABFA assumed that all sources produced steady signals, or at least that received signals could be considered steady over a signal integration (processing) time of the sensor. In signal processing parlance, the received signal statistics were assumed to be *stationary* in time. However, the received signal originating from a moving or transient source varies in time (i.e., is *nonstationary*). Because ABFA performs its calculations in the frequency-domain, it is challenging to develop techniques to accommodate nonstationary signals that are accurate yet not too computationally intensive.

The current version of ABFA allows the received spectrum to vary from one moment in time to the next. The spectrum is considered to result from repeated, short-time Fourier transforms applied at each time interval. So long as this interval is short in comparison to the timescale over which the changes in the received signal occur, the short-time Fourier transform representation is a reasonable one. In this section, we describe how moving and transient source calculations are implemented through this new representation.

5.1 Internal Representation of Nonstationary Sources

The information on each source is stored by ABFA in a structured variable called `SourceInfo`. Previous versions of ABFA included the following among the fields in `SourceInfo`: `xcoord`, the eastward displacement of the source relative to the southwest corner of the computational domain; `ycoord`, the northward displacement of the source relative to the southwest corner of the computational domain; and `zcoord`, the vertical displacement of the source relative to the local terrain elevation. These were all scalar values. ABFA Version 3.0 extends this representation to include the field `tcoord`, which is the time relative to some convenient initiation time. The fields `xcoord`, `ycoord`, `zcoord`, and `tcoord` can all be vectors (of the same length M), representing 4-D coordinates of the source. If $M = 1$, the source is assumed to emit a stationary (constant for all time) signal and the value of `tcoord` has no effect. If $M > 1$, the source is assumed to turn on at `tcoord(1)` and turn off at `tcoord(M)`. The spectral `loudness` field (discussed in Section 4) has been generalized to be an $M \times N$ matrix, where N is the number of frequency bands. If the coordinate fields all have

length M , but the **loudness** field has size $1 \times N$, the source spectrum (but not necessarily the receiver spectrum) is assumed to be stationary, although the source coordinates may vary.

Much of the discussion in the previous paragraph applies to the **RcvrInfo** structure as well, which contains the properties of a receiver. A **tcoord** field has been added and all coordinate fields can be vectors. The extended coordinate fields in **RcvrInfo** allow implementation of moving receivers such as unmanned aerial vehicles (UAVs). However, the **RcvrInfo** contains no counterpart to the **loudness** field. Computational implementation of moving receivers is nearly the same as for moving sources. The main difference is that the principle of acoustic reciprocity (Pierce 1981) is applied (along with a reversal of the wind direction) to convert the moving receiver problem to a moving source problem. This procedure is valid in the presence of refraction by atmospheric wind and temperature gradients and other complications.

5.2 Calculation Method for Nonstationary Sources

As mentioned earlier in this section, previous versions of ABFA assumed that the sound output from the source was steady. The user had the option of calculating the SPL produced by the source. The SPL is defined as (Crocker 1997)

$$L_p = 10 \log_{10} \left(\frac{p_{\text{rms}}^2}{p_{\text{ref}}^2} \right), \quad (7)$$

where p_{rms} is the root-mean-square sound pressure.

For sources that are nonstationary, one can define the *sound exposure* as

$$E = \int_{t_1}^{t_2} p_{\text{rms}}^2(t) dt. \quad (8)$$

The integration limits t_1 and t_2 are normally set to $-\infty$ and ∞ , respectively. The sound exposure level (SEL) is then defined as (Pierce 1981)

$$L_E = 10 \log_{10} \left(\frac{E}{p_{\text{ref}}^2 T_{\text{ref}}} \right), \quad (9)$$

where $T_{\text{ref}} = 1 \text{ s}$ is the reference time interval. Hence, for a sound source that emits a steady sound for a 1-s interval but is otherwise quiet,

$$L_p = L_E.$$

The new version of ABFA includes a capability for calculating L_E . When a user selects (clicks on) a moving or transient source, and then selects “Sound pressure/exposure level” from the Calculation pull-down menu, the

SEL is automatically calculated instead of the SPL. Calculations of L_E (like L_p) may be performed with no frequency weighting, or with an A- or C-weighting network standard in noise control applications (Krug 1997). Users should keep in mind that ABFA's SEL calculation includes only the contribution from the selected source; the contribution from the noise background is not included. If it were, the SEL would become infinite.

The SPL and SEL calculations are primarily useful in noise control applications. In most U.S. Army tactical scenarios, however, a sensor processes a signal for a finite time interval (the sensor integration time) and then reaches a decision or produces a final result. The performance of the sensor is determined by the relative exposure of the sensor to the signal of interest (s) and the noise (n) during the integration time.

Accordingly, it is useful to define a signal exposure as

$$E_s = \int_{t_1}^{t_1+T} s_{\text{rms}}^2(t) dt, \quad (10)$$

and a noise exposure as

$$E_n = \int_{t_1}^{t_1+T} n_{\text{rms}}^2(t) dt, \quad (11)$$

where T is the sensor integration time, and s_{rms} and n_{rms} are the root-mean-square sound pressures due to the source and noise, respectively. The signal-to-noise ratio, expressed in decibels, is then

$$\text{SNR} = 10 \log_{10} \left(\frac{E_s}{E_n} \right). \quad (12)$$

Because the noise level is assumed to be constant (stationary), equation (11) reduces to $E_n = n_{\text{rms}}^2 T$. On the other hand, it would be impractical to implement equation (10) directly into a tactical decision aid such as ABFA. The exact times when the sensor turns on and off would need to be specified, and then the signal-to-noise ratio (SNR) would need to be calculated for each individual processing interval. Most users do not want to analyze a scenario to this level of detail. Hence, a simplified methodology has been developed. This methodology is based on determination of the SNR for two scenarios representing opposite extremes.

Let us illustrate the two extreme scenarios based on a moving source. In the first scenario, the source, when it reaches the portion of its trajectory maximizing the SNR, is moving slowly in comparison to the integration time of the sensor. The SNR is therefore nearly constant during the processing. It would be reasonable to approximate E_s by finding the peak

value of $s_{\text{rms}}^2(t)$ over the source trajectory and then multiplying by T , similarly to how the noise is processed:

$$E_s \simeq \max [s_{\text{rms}}^2(t)] T. \quad (13)$$

In the second scenario, the source moves very rapidly past the sensor, so that the signal level is high only for a small fraction of the integration time. The integration limits in equation (10) become unimportant and one could use the calculation of L_E to determine E_s :

$$E_s \simeq p_{\text{ref}}^2 T_{\text{ref}} 10^{L_E/10}. \quad (14)$$

To estimate the SNR of a processor in the presence of a moving source, ABFA estimates E_s with both of the equations above. It then calculates the SNR using the lesser of the two estimates. This method reduces exactly to the correct results for stationary sources and provides a very good approximation for fast-moving sources.

Transient sources are handled similarly. The first extreme scenario would correspond to a source signal that varies slowly over the sensor integration time. The second extreme scenario would be a transient that starts and finishes well within the integration time.

5.3 Moving Source Implementation

Coordinates for a moving source are loaded from text files. Text files containing relative (in kilometers from the southwest corner of the domain), UTM, and latitude/longitude coordinates are all supported. The files have three required columns and an optional fourth. The first column represents time. It can be a floating point value (which is interpreted as having units of seconds) or any unambiguous date/time format supported by MATLAB's datenum function. The second column is easting (for relative or UTM coordinates) or longitude. The third column is northing (for relative or UTM coordinates) or latitude. The optional fourth column is the source height relative to ground level. This column will be ignored for sources such as ground vehicles that have a fixed height. Support is also provided for GPS coordinate files in ARL's Acoustic Database (Nguyen et al. 1999). These files specify UTM coordinates but have a slightly more complicated format than the one just described.

A moving source (or receiver) is created by first following the usual procedure for adding an object to the terrain display at a fixed location (i.e., going to the Source menu, then to Add, then selecting the desired type, and lastly placing it on the domain with the mouse). Next the user right clicks on the source icon and brings up the properties dialog box. A

pull-down menu at the top of the dialog box displays the method by which the coordinates are currently specified. This is initially set to “Enter fixed coordinates and speed in boxes below.” To load a coordinate text file, select the desired coordinate specification (relative, UTM, or latitude/longitude) from the pull-down menu. ABFA will then prompt for the text file name and load the coordinates. Internally, the new coordinates are converted into relative coordinates (if necessary) and placed into the `SourceInfo` structure. The `loudness` field is not changed, implying that the source spectrum is stationary.

Moving sources are plotted with the source icon (usually an X) at the initial point in the trajectory and an arrow at the termination. A line connects the initial point to the termination. Moving receivers are plotted in the same way, except that the receiver icon (usually a circle) is used at the initial point.

The time steps in the source coordinate specification should be short enough that the received signal energy does not dramatically change from one time step to the next. If the time resolution is not fine enough, there may be no time step close to the location at which the received signal energy is maximized (typically near the point of closest approach to the sensor). ABFA’s calculations of $\max [s_{\text{rms}}^2(t)]$ in equation (13) and L_E in equation (14) will then both be poor, resulting in a poor approximation for the SNR.

An example probability of detection calculation on a moving tracked, armored vehicle is shown in Figure 4. The vehicle track and weather conditions were loaded from an ATR Database trial conducted shortly after midnight on 17 December 1998 at Spesutie Island, APG, MD. (Terrain elevations for this trial are plotted in Figure 2.) In this trial, there was a strong wind of 9.25 m/s blowing from the northeast. According to the ABFA predictions, high wind noise and upward refraction over the water confined the area of detection primarily to the island.

5.4 Transient Source Implementation

Three basic transient signal models (plotted in Figure 5) are presently available.

- *N-wave*. The N-wave represents shocks generated by supersonic aircraft and other sources. It is described internally by the following equation for the sound pressure:

$$p(t) = \begin{cases} A(1 - t/T_p), & 0 \leq t \leq 2T_p, \\ 0, & \text{elsewhere,} \end{cases} \quad (15)$$

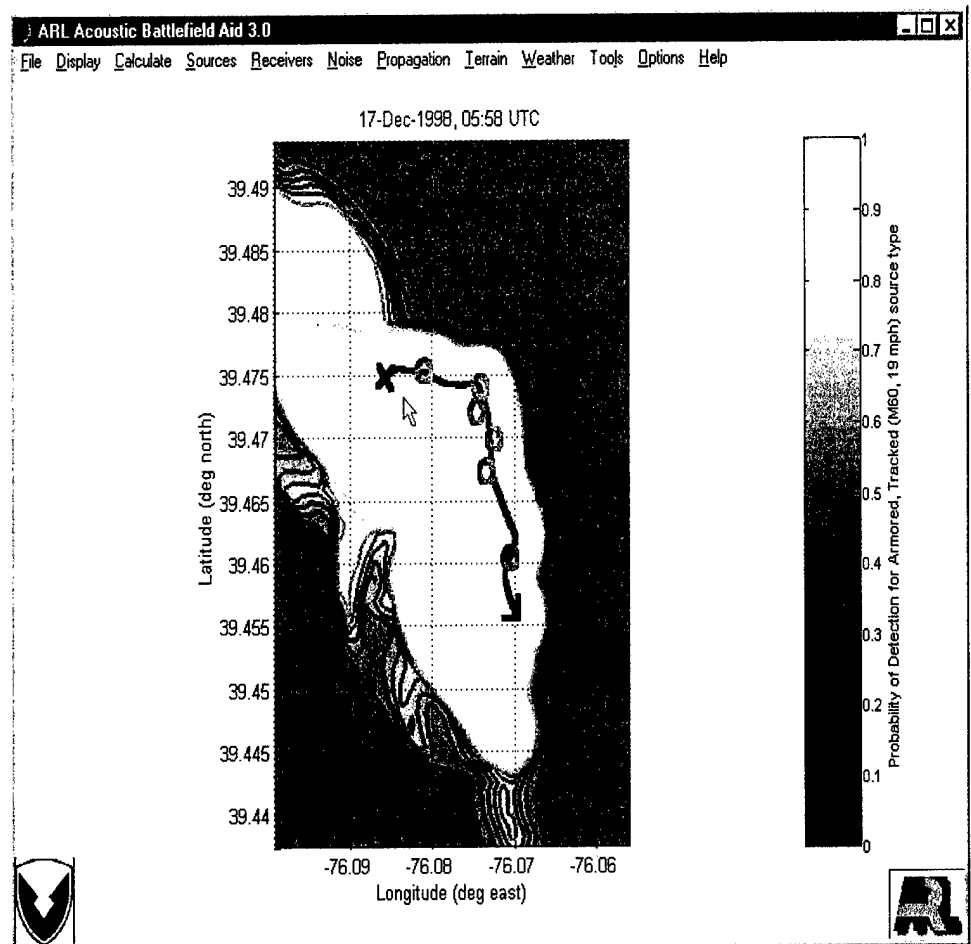


Figure 4. Probability of detection display for a moving source. White represents high probability of detection; medium gray represents near-zero probability of detection.

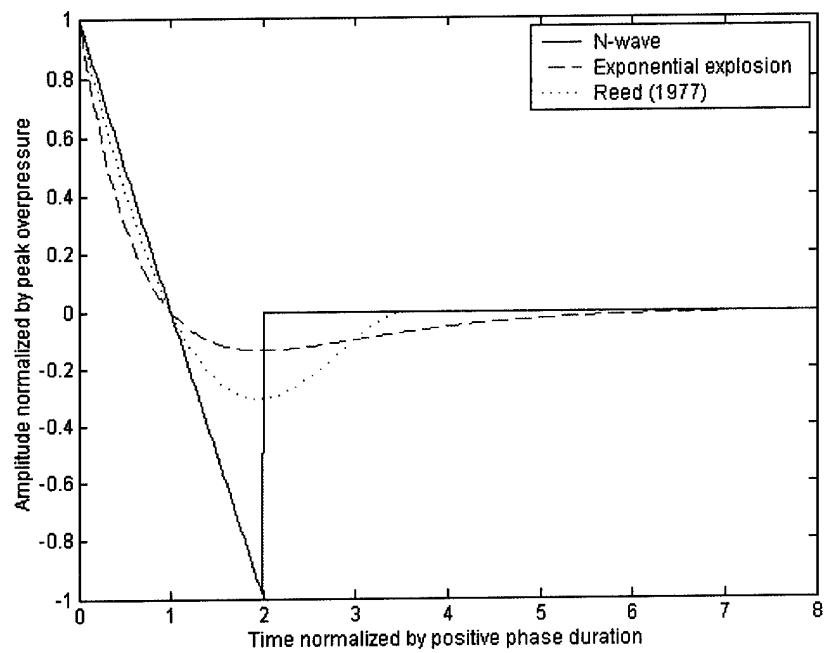


Figure 5. Three representations for shock waves and explosions. Plotted is $p(t)/A$, where A is the peak overpressure. The time axis is normalized by the positive phase duration T_p .

where A is the peak overpressure and T_p is the positive phase duration.

- *Exponentially decaying explosion.* Explosions have often been modeled previously using an exponentially decaying function, described by the following equation:

$$p(t) = \begin{cases} A(1 - t/T_p) \exp(-t/T_p), & 0 \leq t, \\ 0, & \text{elsewhere.} \end{cases} \quad (16)$$

Internally, ABFA cuts off the pressure signal at $t = 8T_p$, setting it equal to zero thereafter. At this time, the pressure has decayed to $-0.0023A$, down from its initial value of A .

- *Reed (1977) explosion model.* Reed (1977) points out that the exponential model poorly describes the negative pressure phase of an explosion and offers the following equation as an alternative:

$$p(t) = \begin{cases} A(1 - t/T_p)(1 - t/T_d)(1 - t^2/T_d^2), & 0 \leq t \leq T_d, \\ 0, & \text{elsewhere,} \end{cases} \quad (17)$$

where T_d is the total pulse duration. To produce a net zero-mean flow condition, T_d is set to $T_p/0.28$ (White 1991).

To accommodate transient signals, a new field was added to the `SourceInfo` called “`OtherParam`”. This field is a MATLAB cell array, whose first element is a string representing the implementing function for the transient (`Nwave`, `ExpExplode`, or `Reed1977`, for the three currently available signal models). The remaining elements of the cell array are arranged in pairs, the first element being a descriptive string for the parameter needed by the implementing function and the second its default value. These additional parameters are listed when the source properties dialog box is opened, and they are sent in order to the implementing function.

The internal coordinate representation of a transient source is initially the same as a source with fixed spatial coordinates, with the fields `tcoord`, `xcoord`, `ycoord`, and `zcoord` of the `SourceInfo` structure all being scalar values. However, the spectral representation (the `loudness` field in `SourceInfo`) is in the FFT bin coefficient format as indicated with a value of -1 for the `OctaveBand` field, as described in Section 4. When a calculation is started, ABFA converts the `SourceInfo` to a representation similar to that of a moving source. The conversion process is driven by the sensor’s signal integration time. If the integration time is larger than the length of the transient, then the spectrum of the transient is passed

without alteration. In this case, equation (14) will be used to determine the SNR. If the integration time is shorter than the length of the transient, the transient will be divided into M blocks having (as closely as possible) the same duration as the sensor integration time. The spectrum of each of these blocks is then put into an $M \times N$ **loudness** field, and the coordinate arrays of **SourceInfo** are expanded into M -element vectors. The spatial coordinates are repeated, although **tcoord** steps forward in increments of the sensor integration time. Generally equation (13) will be selected to calculate the SNR.

This approach to calculations with transients may not be satisfactory if there are strong multipaths whose separation in time is longer than the receiver's integration time. But in situations where the system performance is dominated by a single propagation path or closely spaced multipaths, it is a very reasonable approach. When performing calculations on transient signals, the minimum frequency in ABFA's propagation table should be set to a very low value (e.g., 1 Hz). This is because transients often contain strong signal energy down to very low frequencies. If the minimum frequency in the propagation table is not low enough, extensive extrapolation of the table will occur. This could result in very poor transmission loss predictions.

ABFA's AWAUI (Wilson and Szeto 2000) was modified to plot transient signals. When AWAUI is invoked to analyze sound recordings (through the wizards for creating new source and background noise types), it provides the option of saving the spectrum in the FFT bin coefficient format so that calculations can be later performed on the transient signal.

6. Java Weather Interface

MATLAB Versions 6.0 and 6.1 support embedded Java commands. ABFA uses this capability to provide users with access to several Internet sources of weather data, by sending sequences of FTP and HTML instructions. The Web sites are:

- *National Weather Service Internet Weather Source (IWS),* [*http://weather.noaa.gov/weather/metar.shtml*](http://weather.noaa.gov/weather/metar.shtml). This site contains worldwide METAR (Aviation Routine Weather Report) messages updated at hourly intervals. These messages are highly condensed text files containing information such as surface wind speed and direction, surface temperature, surface relative humidity, and cloud cover. They are accessed in ABFA by entering the four-letter ICAO (International Civil Aviation Organization) code of the weather station of interest. Alternatively, ABFA will search a list of available stations to find the ones closest to the current computational domain and then prompt the user to select the station of interest. After downloading and parsing the METAR message, a surface-energy balance model (Wilson and Szeto 2000) is then invoked to determine the near-ground vertical profiles of wind, temperature, and humidity, as well as turbulence parameters used to calculate sound-field saturation and coherence.
- *National Oceanic and Atmospheric Administration Realtime Environmental Applications Display sYstem (READY),* [*http://www.arl.noaa.gov/ready/cmet.html*](http://www.arl.noaa.gov/ready/cmet.html). Numerical weather forecasts from a large number of atmospheric models are collected at this site. ABFA currently provides access to data from the Medium-Range Forecast (MRF) model, which covers the northern hemisphere, and from the lower resolution Aviation (AVN) model, which covers the entire globe. (Several other forecast models are available at this Web site, and access to these could be added in the future.) Access to the MRF and AVN models works in the same way: ABFA first requests the forecast data for the latitude and longitude of the origin (southwest corner) of the current computational domain. The READY Web site then interpolates the coarse-resolution forecast model data to this particular location. The resulting vertical profiles of wind, temperature, and humidity are

then pushed to ABFA. Generally, these profiles do not have sufficient resolution to accurately predict sound refraction near the ground. Therefore, ABFA provides an option of invoking Monin-Obukhov similarity to estimate profiles at a higher resolution within the atmospheric surface layer, based on the values of the forecast profiles at the lowermost two grid levels.

- *National Oceanic and Atmospheric Administration (NOAA) Forecast Systems Laboratory (FSL) Web Site*, *http://maps.fsl.noaa.gov/newmain.html*. Access is provided to the RUC (Rapid Update Cycle) and MAPS (Mesoscale Atmospheric Prediction System). These forecasts cover the United States at 20–40 km resolution. Forecasts out to 24 hrs in advance are updated every 3 hrs. ABFA also accesses the radiosonde soundings collected at this Web site. Soundings from major airports are available, being accessed by their four-letter ICAO code. The process of retrieving the profiles for any of these data resources is similar to the READY Web site retrieval. The option estimating the profiles at higher resolution in the atmospheric surface layer using Monin-Obukhov similarity is also provided.

In addition, ABFA can load data stored on the local computer in several text-file formats. Supported formats currently include: METAR messages, the ARL SCAFFIP (SCAnning Fast FIeld Program) format, the Army IMETS (Integrated METeorological System) UAMET format, and the Navy standard upper-air sounding format. Processing of the locally stored METAR messages is done in the same manner as when they are downloaded over the Internet. The SCAFFIP, UAMETS, and Navy formats, being full vertical profiles, are processed in the same way as the NOAA/READY and NOAA/FSL forecast data.

7. Dependence of Sound Speed on Atmospheric Humidity

Water vapor in the atmosphere affects sound waves in two primary ways: it alters the attenuation (dissipation as heat) of propagating sound energy and modifies the refractive characteristics of the air through the dependence of the sound speed on air density. The former effect was accounted for in earlier versions of ABFA. Users specified a single value of the relative humidity that was subsequently used by the program to calculate the attenuation coefficient. In the new version, the full vertical profile of humidity is stored in the same manner as the temperature and wind profiles for subsequent calculation of both the attenuation and sound speed. As a result, the height-dependence of absorption and refraction by humidity gradients are now included in calculations.

Several derivations of the dependence of sound speed on temperature and humidity can be found in the literature, many of which contain errors or values of constants that are inaccurate. Here a concise derivation is presented that leads to the correct dependence of the sound speed on humidity. It is based on the derivation in Pierce (1981).

For an ideal gas, it is well known that

$$c = \sqrt{\gamma RT}. \quad (18)$$

Here, $\gamma = C_p/C_v$ is the specific heat ratio, $R = R_0/M$, where $R_0 = 8314 \text{ m}^2 \text{ s}^{-2} \text{ K}^{-1}$ is the universal gas constant and M is the average molecular mass. Note that for an ideal gas, the speed of sound is independent of pressure. Air is a mixture consisting primarily of diatomic nitrogen, diatomic oxygen, monatomic argon, and water vapor. The amount of water vapor is highly variable, whereas the proportions of the other constituents are nearly constant. The average molecular mass of moist air, weighted by fraction, is simply

$$M = (1 - h) M_d + h M_w, \quad (19)$$

where the subscript d indicates dry air, w indicates water vapor, and h is the fraction of molecules that are water vapor. The molecular mass of dry air is $M_d = 28.96$, whereas the molecular mass of water vapor M_w is 18.02 .*

The specific heat ratio can be deduced from the structure of the constituent molecules. According to the kinetic theory of gases, $C_v = (R/2)(T + F)$,

*Values for molecular masses in this section are taken from Table 1 in Zuckerwar (1997).

where T is the number of translational degrees of freedom of the molecule (always 3) and F is the number of rotational degrees of freedom Zuckerwar (1997). The relationship $C_p = C_v + R$ then yields $\gamma = (5 + F) / (3 + F)$. Water molecules have an additional rotational degree of freedom in comparison to diatomic molecules so that $F = 2 + h$ in the mixture, and

$$\gamma = \frac{5 + 2(1 - h) + 3h}{3 + 2(1 - h) + 3h} = \frac{7 + h}{5 + h}. \quad (20)$$

In deriving this result, the contribution of argon and other trace constituents in the air has been neglected.

The range of values for h in the atmosphere is about 0 to 0.04 Wallace and Hobbs (1977). Since $h \ll 1$, it is reasonable to expand equations (19) and (20) in powers of h and neglect terms of order h^2 and higher, resulting in

$$R = R_d [1 + (1 - \varepsilon) h], \quad \gamma = \gamma_d \left(1 - \frac{2h}{35}\right), \quad (21)$$

where $\varepsilon = M_w/M_d = 0.6222$. Now, by substitution into equation 18, we have for moist air

$$c = \sqrt{\gamma_d R_d T [1 + (33/35 - \varepsilon) h]} \simeq 20.05 \sqrt{T} (1 + 0.160h). \quad (22)$$

Therefore, the presence of water vapor increases the gas constant but decreases the specific heat. The effect of the vapor on the gas constant is more significant, causing the sound speed to increase.

The molecular-fraction humidity h , while convenient for describing the dependence of sound speed on water vapor, is not often used by atmospheric scientists. Internally ABFA quantifies the humidity with the specific humidity (q), defined as the mass of water vapor divided by the total mass of air in a sample. The specific humidity relates to h as follows:

$$q = \frac{hM_w}{hM_w + (1 - h)M_d} = \frac{\varepsilon h}{1 + (\varepsilon - 1)h}. \quad (23)$$

With $h \ll 1$, this relationship implies that q is approximated by εh to first order in h . Hence, equation (22), in terms of the specific humidity, becomes

$$c = \sqrt{\gamma_d R_d T (1 + \eta q)} \simeq 20.05 \sqrt{T} (1 + \eta q/2), \quad (24)$$

where

$$\eta = \frac{33}{35\varepsilon} - 1 = 0.515. \quad (25)$$

The second result in equation (24) follows from a Taylor series expansion to first order in q . Frequently in practice, the relative humidity is specified

instead of specific humidity. Therefore ABFA includes routines to convert between these two humidity measures. The conversion is based on the well-known Goff-Gratsch equation (Goff 1965).

Because $q \ll 1$, the contribution of humidity to the actual sound speed is usually small. But this does not necessarily mean that the effect of humidity is unimportant for propagation in general. Many propagation phenomena, such as refraction and scattering, depend on *contrasts* between the sound speed at different locations in the atmosphere. Therefore, it is the deviations of the temperature and humidity from some background state that are important. Let us write $T = T_0 + T'$ and $q = q_0 + q'$, where T_0 and q_0 are reference values for the temperature and humidity (for example the means at a fixed height), and T' and q' are presumed small perturbations. Substituting these expansions into equation (24) yields

$$c = c_0 \sqrt{\left(1 + \frac{T'}{T_0}\right) \left(1 + \frac{\eta q'}{1 + \eta q_0}\right)}, \quad (26)$$

where

$$c_0 = \sqrt{\gamma_a R_a T_0 (1 + \eta q_0)}. \quad (27)$$

Keeping only the first-order contributions in T' , q' , and q_0 , one has $c = c_0 + c'$, where

$$c' \simeq \frac{c_0}{2} \left(\frac{T'}{T_0} + \eta q' \right). \quad (28)$$

Based on equation (28), with the reference values T_0 and q_0 taken to be independent of height, the vertical gradient is

$$\frac{\partial c}{\partial z} = \frac{\partial c'}{\partial z} = \frac{c_0}{2} \left(\frac{1}{T_0} \frac{\partial T'}{\partial z} + \eta \frac{\partial q'}{\partial z} \right). \quad (29)$$

When Monin-Obukhov similarity (e.g., Stull 1988) is invoked to model the vertical sound-speed profile (i.e., when the user does not specify the temperature and humidity profiles directly), the following equation applies to the vertical gradient

$$\frac{\partial c}{\partial z} = -\frac{\Gamma_d c_0}{2T_0} + \frac{P_t c_*}{k} \phi_h \left(\frac{z}{L_o} \right), \quad (30)$$

where $\Gamma_d = 0.0098 \text{ } ^\circ\text{K/m}$ is the dry adiabatic lapse rate (accounting for the decrease of temperature with height due to compression in the air column), $k = 0.40$ is von Kármán's constant, $P_t = 0.95$ is the turbulent Prandtl number, ϕ_h is a presumed universal gradient function, and L_o is Obukhov's

lengthscale, which is described in texts on boundary-layer meteorology such as Stull (1988). The quantity c_* is a sound-speed fluctuation scale, given by

$$c_* = \frac{c_0}{2} \left(\frac{T_*}{T_0} + \eta q_* \right), \quad (31)$$

where $T_* = -\langle w'T' \rangle_s / u_*$ and $q_* = -\langle w'q' \rangle_s / u_*$, with u_* being the friction velocity and $\langle w'\xi' \rangle_s$ the vertical kinematic flux of the quantity ξ at the surface. The following form for the profile function ϕ_h , based on results in Högström (1996) and Wilson (2001), is used by ABFA:

$$\phi_h(\zeta) = \begin{cases} (1 + 7.9|\zeta|^{2/3})^{-1/2}, & \zeta < 0 \\ 1 + 8.4\zeta, & \zeta \geq 0 \end{cases}, \quad (32)$$

In writing equation (30), it was assumed that the potential temperature and humidity gradients are both proportional to ϕ_h . Integrating equation (30), the result is

$$c(z) = c(z_r) - \frac{\Gamma_d c_0 z}{2T_0} + \frac{P_t c_*}{k} \left[\ln \frac{z}{z_r} - \Psi_h \left(\frac{z}{L_o} \right) + \Psi_h \left(\frac{z_r}{L_o} \right) \right], \quad (33)$$

where z_r is a reference height at which the temperature and humidity are known (typically 2 m), and

$$\Psi_h(\zeta) = \begin{cases} 2 \ln [(1 + (1 + 7.9|\zeta|^{2/3})^{1/2})/2], & \zeta < 0 \\ -8.4\zeta, & \zeta \geq 0 \end{cases}. \quad (34)$$

8. Ground Parameter Menu

A new ground parameter menu (Figure 6) was designed to provide immediate feedback to users as the parameters are changed. The ground parameters are separated into three classes: acoustical properties, radiative properties, and aerodynamics properties.

The acoustical properties (flow resistivity, porosity, tortuosity, and pore shape factor) determine the ground impedance and complex wavenumber used by the propagation models. Calculation of these quantities is based on a viscous and thermal relaxational model (Wilson 1997). When the acoustical properties are changed, plots of the reflection coefficient and surface impedance (normalized by the product of the sound speed and density of air) are automatically updated.

The radiative properties (surface albedo and Bowen ratio) are used internally by a surface-energy balance model (Wilson and Szeto 2000) to determine the fluxes of sensible and latent heat at the ground. The fluxes are needed to calculate the temperature and humidity profiles near the ground, unless these profiles are specified directly by the user. When the Bowen ratio (ratio of the sensible to the latent heat flux) is changed, a graphical display of the flux partitioning (shown in the upper middle of Figure 6) is automatically updated. Because the flux partitioning schemes differ at day and night, a pair of radio buttons are supplied that allow the user to toggle between the two schemes. The surface albedo (fraction of incoming shortwave solar radiation that is reflected by the ground) has no effect on the flux partitioning plot, although it does affect the temperature profile.

The aerodynamic properties (roughness and displacement heights) primarily affect the wind profile near the ground. A display of the wind profile, as it would in neutral atmospheric conditions, is updated when the user changes these properties. This display is determined from the following logarithmic form for the vertical wind profile, which is valid in neutral conditions (e.g., Stull 1988):

$$U(z) = \frac{u_*}{0.4z} \ln \left(\frac{z - d}{z_0} \right), \quad (35)$$

where u_* is the friction velocity, z_0 is the surface roughness, and d is the displacement height. Therefore, the ratio of $U(z)$ to its value at some

normalization height z_n is

$$\frac{U(z)}{U(z_n)} = \frac{\ln [(z - d) / z_0]}{\ln [(z_n - d) / z_0]}, \quad (36)$$

which is independent of u_* . As the user changes the values of z_0 and d , the plot of the ratio $U(z) / U(z_n)$ on the right side of the display is updated. The value of z_n is internally set by the program to produce a good plot. Note that ABFA does not generally use neutral conditions in its calculations; the purpose of the wind-profile plot in the ground parameter menu is simply to provide informative feedback to the users as they change the aerodynamic properties. The actual wind profile to be used in calculations can be plotted from the Weather pull-down menu.

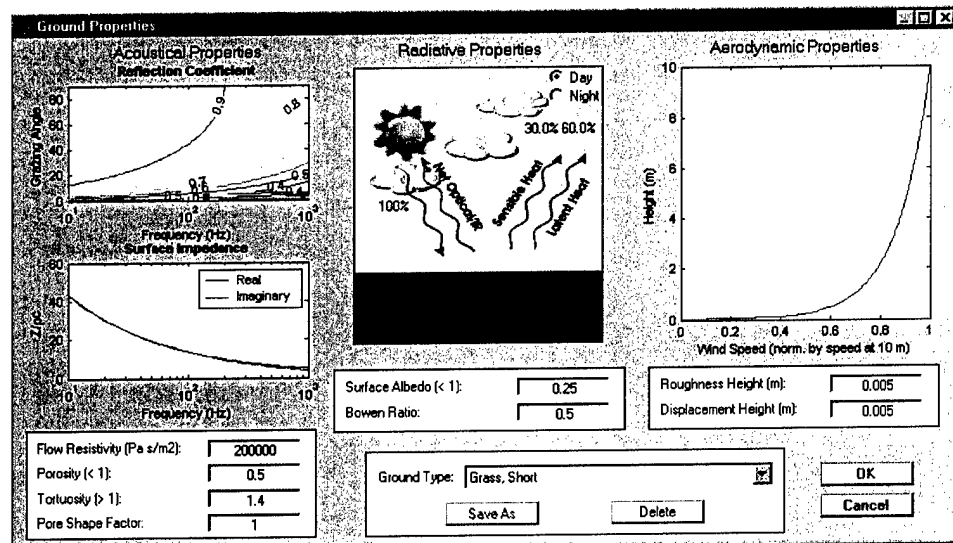


Figure 6. Ground parameter menu.

The name of the current ground type is shown on a pull-down list near the bottom of the ground parameters menu. The ground type can be changed simply by selecting a new name from the list. The parameter values are then updated. Whenever a user changes any of the ground parameters manually, the ground type name becomes "custom" and the "Save As" button is activated. By clicking on "Save As," the modified ground parameters can be saved under a new name. This name will subsequently appear on the ground type pull-down list. Existing ground types can be deleted by selecting them from the pull-down list and then clicking the "Delete" key.

9. Creation of an ABFA Windows Executable

One of the limitations of the ABFA code in Versions 2.5 and prior was that MATLAB was required to run it. A MATLAB license with the signal processing and mapping toolboxes costs several thousand dollars.

Therefore, it is highly desirable to find a way to distribute the code that will not require users to obtain MATLAB. Fortunately, in recent years The MathWorks, Inc. (the developers of MATLAB) has developed a compiler that converts MATLAB source code to C or C++ code (The MathWorks, Inc. 2000). Supplementing the compiler are libraries containing object code for MATLAB graphical and mathematical functions. Most features of interpreted (command line) MATLAB are supported by the compiler and object libraries.

We have succeeded in creating an executable version of ABFA that retains nearly all of the functionality of the MATLAB interpreted code. The only significant difference is that the Java capability for accessing weather data on the Internet is not supported by the compiler. Several other changes to the original ABFA code were found necessary to produce the executable, although these are transparent to users. The main changes were:

- Callbacks (commands that are launched from user-interface controls such as buttons) had to be rewritten to execute from MATLAB functions rather than the MATLAB interpreter command line. To accomplish this, many of the variables that are stored in the main workspace when ABFA runs were declared at the beginning of the code as global variables. The callback functions then access these global variables.
- The compiler supports only forms of the MATLAB `load` and `save` commands that explicitly provide the names of the variables being loaded or saved. Conversion of the `load` and `save` commands in ABFA to these forms was not difficult.
- Many ABFA functions tested for the presence of input arguments using the MATLAB `exist` command. However, the compiler does not support this usage. This usage of `exist` was easily replaced by tests based on the `nargin` variable. Similarly, in some instances ABFA used the `exist` command to determine whether files were present. This usage was replaced by an `fopen` command; the value returned by `fopen` is examined to determine whether the file was present.

- The MATLAB `eval` command, which is unsupported by the compiler, was used by ABFA in several instances. All were easily replaced by the MATLAB `feval` command, which allows functions to be called with the name of the function determined at runtime.
- As mentioned earlier, the MATLAB compiler does not presently support Java commands. Routines containing Java commands were therefore replaced (in the compiled version of ABFA only) by “place-holder” routines that do not include the Java functionality.

Generally speaking, the executable version of ABFA runs faster than the interpreted MATLAB code. This is particularly so for graphical processes. The sound propagation calculations exhibit only modest speed improvements.

10. Concluding Remarks and Future Recommendations

The ABFA enhancements described in this report, such as calculations with moving/transient sources, a meteorological data interface, and map displays generated from digitized feature data, significantly improve the program's utility in both operational and research settings. To a great extent, the original goal of the ABFA program, to make the current generation of advanced sound propagation models conveniently available for realistic battlefield acoustic and noise impact predictions, has been now realized. Nonetheless, there are still many worthwhile improvements that could be made. Four such improvements recommended here for future consideration are as follows:

1. *Extension of the library of source (target) signatures.* Currently, the signature library is rather small (with about 25 signatures) and consists primarily of tracked ground vehicles. The signatures also have a low resolution in the frequency domain. It would be desirable to extend the library, in particular with regard to aircraft. Interfacing the program with source models, such as the recently developed DOD acoustic helicopter model, should be considered.
2. *Development of an expert system for setting the propagation table parameters.* Users experienced in outdoor sound propagation generally recognize how to set the propagation table parameters appropriately. However, this task is much more challenging for non-experts.
3. *Calculations of seismic sensor performance.* Many U.S. Army platforms having acoustic sensors also have seismic ones. Much of the functionality and organization of the ABFA program would be well suited to seismics. Additional propagation models would need to be introduced into the program, along with graphical user-interface structures to set up the positions of the seismic sensors and the ground elastic properties.
4. *Assimilation of meteorological data from multiple sources.* Currently, ABFA accesses weather data from only one data source at a time. The data source could be either surface weather observations or a set of vertical profiles. It would be desirable to have capabilities for merging weather data from a variety of sources. For example,

low-resolution global forecast data could be merged with local surface data or soundings. Development of tools for accomplishing tasks such as this is currently an active area of atmospheric research, and ABFA might be able to take advantage of the recent progress.

Acknowledgments

Most of the improvements described in this report were carried out with funding from the National Ground Intelligence Center, administered by Robert Grachus. Funding from a U.S. Army Research Laboratory (ARL) Director's Research Initiative, "Modeling Battlefield Acoustic Detection by Advanced ATR Algorithms and the Human Auditory System," supported development of the interface between the Acoustic Battlefield Aid (ABFA) and the Automatic Target Recognition (ATR) Acoustic Database.

The Java-based capability for retrieving weather data over the Internet was developed primarily by Bruce VanAartsen of TASC/Litton, under contract from ARL. The original capability for initializing ABFA from the ATR Acoustic Database was developed by Greg Szeto, a student in the Science Engineering and Apprenticeship Program (SEAP) administered by George Washington University. Most of the graphical user-interface for ground parameters was developed by Meredith Hutchinson, also a SEAP student. We furthermore thank Steve Tenney and Alan Wetmore for their helpful discussions on geographical information sources and other topics.

In Memoriam. One of the authors of this report, Anh Nguyen, passed away while this work was in progress. The U.S. Army acoustical community lost one of its most dedicated and skilled software developers. We greatly miss our quiet and kind colleague.

Bibliography

Crocker, M. J. (1997): Introduction. In *Encyclopedia of Acoustics*, Crocker, M. J., editor, volume 1, Wiley-Interscience, New York, 3–19.

Goff, J. A. (1965): Saturation pressure of water on the new Kelvin scale. In *Fundamentals and Standards of Humidity and Moisture: Measurement and Control in Science and Industry*, Wexler, A., editor, volume 3. Reinhold, New York.

Högström, U. (1996): Review of some basic characteristics of the atmospheric surface layer. *Boundary-Layer Meteorol.*, **78**, 215–246.

Krug, R. W. (1997): Sound level meters. In *Encyclopedia of Acoustics*, Crocker, M. J., editor, volume 1, Wiley-Interscience, New York, 1845–1854.

Nguyen, V. A., H. Vu, and L. Sim (1999): An overview of ARL's Acoustic Database. Technical Report ARL-TR-1832, U.S. Army Research Laboratory, 2800 Powder Mill Road, Adelphi, MD 20783.

Pierce, A. D. (1981): *Acoustics: An Introduction to Its Physical Principles and Applications*. McGraw-Hill, New York.

Reed, J. W. (1977): Atmospheric attenuation of explosion waves. *J. Acoust. Soc. Am.*, **61**, 39–47.

Stull, R. B. (1988): *An Introduction to Boundary Layer Meteorology*. Kluwer, Dordrecht, Germany.

The MathWorks, Inc. (2000): *Using MATLAB, Version 6*. The MathWorks, Inc., Natick, Massachusetts.

Wallace, J. M. and P. V. Hobbs (1977): *Atmospheric Science: An Introductory Survey*. Academic Press, New York.

White, M. J. (1991): Personal notes.

Wilson, D. K. (1997): Simple, relaxational models for the acoustical properties of porous media. *Appl. Acoust.*, **50**, 171–188.

Wilson, D. K. (1998): A prototype acoustic battlefield decision aid incorporating atmospheric effects and arbitrary sensor layouts. Technical Report ARL-TR-1708, U.S. Army Research Laboratory, 2800 Powder Mill Road, Adelphi, MD 20783.

Wilson, D. K. (2001): An alternative function for the wind and temperature gradients in unstable surface layers. *Boundary-Layer Meteorol.*, **99**, 151–158.

Wilson, D. K., J. T. Kalb, and N. Srour (2002): Modeling battlefield acoustic detection by advanced ATR algorithms and the human auditory system. Technical Report (to appear), U.S. Army Research Laboratory, 2800 Powder Mill Road, Adelphi, MD 20783.

Wilson, D. K. and G. L. Szeto (2000): Reference guide for the Acoustic Battlefield Aid (ABFA) Version 2. Technical Report ARL-TR-1708, U.S. Army Research Laboratory, 2800 Powder Mill Road, Adelphi, MD 20783.

Zuckerwar, A. J. (1997): Speed of sound in fluids. In *Encyclopedia of Acoustics*, Crocker, M. J., editor, volume 1. Wiley & Sons, 69–79.

REPORT DOCUMENTATION PAGE			<i>Form Approved OMB No. 0704-0188</i>
<p>Public reporting burden for this collection of information is estimated to average 1 hour per response, including the time for reviewing instructions, searching existing data sources, gathering and maintaining the data needed, and completing and reviewing the collection of information. Send comments regarding this burden estimate or any other aspect of this collection of information, including suggestions for reducing this burden, to Washington Headquarters Services, Directorate for Information Operations and Reports, 1215 Jefferson Davis Highway, Suite 1204, Arlington, VA 22202-4302, and to the Office of Management and Budget, Paperwork Reduction Project (0704-0188), Washington, DC 20503.</p>			
1. AGENCY USE ONLY (Leave blank)	2. REPORT DATE	3. REPORT TYPE AND DATES COVERED	
	August 2002	Final, 7/1/01-1/15/02	
4. TITLE AND SUBTITLE Sound Exposure Calculations for Transient Events and Other Improvements to an Acoustical Tactical Decision Aid			5. FUNDING NUMBERS DA PR: AH71 PE: 62784A
6. AUTHOR(S) D. Keith Wilson, V. Anh Nguyen, Nassy Srour, and John Noble			
7. PERFORMING ORGANIZATION NAME(S) AND ADDRESS(ES) U.S. Army Research Laboratory Attn: AMSRL- CI-EE 2800 Powder Mill Road Adelphi, MD 20783-1197			8. PERFORMING ORGANIZATION REPORT NUMBER ARL-TR-2757
9. SPONSORING/MONITORING AGENCY NAME(S) AND ADDRESS(ES) National Ground Intelligence Center 220 Seventh Street NE Charlottesville, VA 22902-5396			10. SPONSORING/MONITORING AGENCY REPORT NUMBER
11. SUPPLEMENTARY NOTES ARL PR: 2FEH26 AMS code: 622784H7111			
12a. DISTRIBUTION/AVAILABILITY STATEMENT Approved for public release; distribution unlimited.			12b. DISTRIBUTION CODE
13. ABSTRACT (Maximum 200 words) Recent enhancements to an acoustical tactical decision aid, called the Acoustic Battlefield Aid (ABFA), are described. ABFA predicts the effects of the atmosphere and local terrain on the performance of acoustical sensors, using advanced sound propagation models. Among the enhancements are (1) sound-exposure and detection calculations for moving and transient sources, (2) new display capabilities including loading of vector-map features from CDs, (3) an interactive menu for entering and managing acoustical and meteorological ground properties, (4) initialization of runs from field trials stored in the U.S. Army Research Laboratory's Automatic Target Recognition Database, (5) a Java-based interface to numerical weather forecast data over the Internet, and (6) creation of a Windows executable version using the Matlab compiler.			
14. SUBJECT TERMS Sound propagation, acoustic sensors, geographical information systems			15. NUMBER OF PAGES 44
			16. PRICE CODE
17. SECURITY CLASSIFICATION OF REPORT Unclassified	18. SECURITY CLASSIFICATION OF THIS PAGE Unclassified	19. SECURITY CLASSIFICATION OF ABSTRACT Unclassified	20. LIMITATION OF ABSTRACT SAR